

A new injectable *in situ* forming hydroxyapatite and thermosensitive chitosan gel promoted by Na₂CO₃

Cite this: DOI: 10.1039/c3sm52508b

Fangfang Li,^a Yang Liu,^a Yun Ding^{*a} and Qiufei Xie^{*b}

A new injectable *in situ* forming hydroxyapatite and thermosensitive chitosan gel (chitosan/HA/Na₂CO₃ gel) promoted by Na₂CO₃ was preliminarily synthesized. This study was the first to use Na₂CO₃ as coagulant to construct the chitosan thermosensitive gel. The sol–gel phase transition, degradation, and morphology of the gel were examined. We found that chitosan/HA/Na₂CO₃ sol with 1.4% Na₂CO₃ has a suitable gelation time (9 min) and degradation rate. SEM images of the dried gel show a porous netlike framework. TEM, EDS, and XRD were combined to confirm the presence of hydroxyapatite. *In vitro* cell culture was performed by using rat bone mesenchymal stem cells (rBMSCs). rBMSCs survived well on the chitosan gel scaffold that formed *in vitro* and *in vivo*, indicating that the chitosan gel was a suitable substrate for the attachment and proliferation of rBMSCs. Subcutaneous implantation of the chitosan gel formed *in situ* into a nude mouse revealed that the chitosan gel loaded with rBMSCs could lead to angiogenesis.

Received 25th September 2013
Accepted 29th December 2013

DOI: 10.1039/c3sm52508b

www.rsc.org/softmatter

1 Introduction

A prospective method for bone repair or regeneration is bone tissue engineering. Bone tissue engineering aims to induce regeneration of functional bone by a synergistic combination of biomaterials, cells, and factor therapy. The development of biomimetic materials has long been a major goal in the field of bone tissue engineering. In order to be suitable for use in clinical therapy, bone cements must possess proper injectability, short setting time, appropriate stiffness, bioactivity, low setting temperature, and radiopacity.¹ Various hydrogels and microspheres have been employed as injectable scaffolds for a variety of biomedical applications.^{2–6} In the last decade, injectable and degradable hydrogels that are formed *in situ* after injection at the defect site have received much attention.^{7–10}

Chitosan is an aminopolysaccharide derived from the deacetylation of chitin, the main structural component of crustacean exoskeletons. This natural and abundant polymer has been used as a scaffolding biomaterial because of its intrinsic antibacterial activity, wound-healing properties, and low immunogenicity.^{11,12} In bone tissue engineering, chitosan has been combined with other materials such as calcium phosphate¹³ and collagen type I¹⁴ to create bioactive composites that enhance mineralization and are potential matrices for cell encapsulation. Chitosan composites also increase bone remodeling in drilled cartilage defects and are promising as

artificial extracellular matrices for cartilage tissue engineering.¹⁵

Since Chenite¹⁶ invented in 2000 a novel, thermally sensitive, and neutral solution from biodegradable gels based on chitosan/ β -glycerophosphate (β -GP) formed *in situ*, most studies have focused on various ratios of chitosan and β -GP or chitosan/ β -GP hydrogels encapsulated in cells.^{17,18} Injectable chitosan hydrogels have been prepared by either physical or chemical cross-linking methods.

Natural bone is a complex inorganic–organic nanocomposite in which hydroxyapatite (HA, Ca₁₀(PO₄)₆(OH)₂) nanocrystallites and collagen fibrils are well organized in a hierarchical architecture over several length scales.^{19,20} Thus, the main way to develop biomaterials as bone substitutes in biomimetic approaches is the construction of nanocrystallites of calcium phosphate (CaP) salts²¹ such as HA dispersed in polymer matrices.

It has been reported that chitosan/HA composites have good biocompatibility and favorable bonding ability with surrounding host tissues.^{22,23} It has also been proved that chitosan/HA composites can further enhance tissue regenerative efficacy and osteoconductivity.^{24,25} The approaches currently used to obtain chitosan/HA composite materials are based on mechanical mixing,²⁶ coprecipitation^{27,28} and an alternate soaking process.^{29,30} A one-step method was used to prepare nanostructured composites from alginate and calcium carbonate or calcium phosphate.³¹

In the present study, we synthesized a new injectable *in situ* forming hydroxyapatite and thermosensitive chitosan gel promoted by Na₂CO₃. The functions of chitosan gels as injectable cell delivery carriers for bone regeneration were evaluated in terms of gelation time, hydrogel stability, and framework.

^aCenter of the Third Clinical, Peking University School and Hospital of Stomatology, Beijing 100191, P.R. China. E-mail: yunding666@126.com; Fax: +86 010 82037073; Tel: +86 010 82037073

^bDepartment of Prosthodontics, Peking University School and Hospital of Stomatology, Beijing 100081, P.R. China. E-mail: xieqiuf@163.com; Fax: +86 010 82195630; Tel: +86 010 82195630

Transmission electron microscopy (TEM), energy-dispersive X-ray spectroscopy (EDS), and X-ray diffraction (XRD) were combined to confirm the presence of hydroxyapatite. *In vitro* cell culture of rat bone marrow mesenchymal stem cells (rBMSCs) using the chitosan gels was carried out to estimate their biological activities, namely, cell compatibility and cytotoxicity. We preliminarily induced bone formation *in vivo* by seeding a scaffold that forms gel *in situ* in the presence of rBMSCs and osteogenic factors. Finally, we evaluated the *in vivo* host tissue responses to rBMSCs containing chitosan gels.

2 Materials and methods

2.1 Preparation of an injectable HA and thermosensitive chitosan gel formed *in situ*

KH_2PO_4 (21.5 mg) and CaCl_2 (30 mg) were mixed with 4 mL of 0.1 M acetic acid solution in distilled water (Milli-Q, USA). Chitosan (100 mg, medium viscosity, 75–80% deacetylated; Aldrich, MI, USA) was dissolved in the above solution, which was then stirred gently for 5 min by using a glass rod (chitosan/HA solution). The initial chitosan concentration was 2.5% (w/v). Various amounts of Na_2CO_3 (70, 80, and 90 mg) were dissolved separately in 1 mL portions of 0.1 M acetic acid solution. To produce the experimental mixtures (chitosan/HA/ Na_2CO_3 sol), 1 mL of the appropriate Na_2CO_3 solution was added to 4 mL of chitosan/HA mixture. The final chitosan concentration was 2% (w/v) and the final Na_2CO_3 concentrations were 1.4%, 1.6%, and 1.8% (w/v). Afterward, the experimental mixtures were stirred gently to yield an elastic, ideal, and thermosensitive chitosan gel (chitosan/HA/ Na_2CO_3 gel) (see Fig. 1).

2.2 Gelation time and degradation *in vitro*

Gelation time. The sol–gel transition behavior was determined by test-tube inversion at 37 °C.³² Chitosan/HA/ Na_2CO_3 sol (1 mL) in a 5 mL vial with a 10 mm inner diameter was prepared. The vials were immersed in a 37 °C water bath. The sol–gel transition temperature was monitored by inverting the

vials every minute; absence of flow in 20 s signaled the formation of a gel.

Degradation. A set of 5 mL vials were weighed (W_v : weight of vial) before use. Chitosan/HA/ Na_2CO_3 gel samples (1 mL) in 5 mL vials were prepared according to the procedure described in Section 2.1, and were kept for 30 min in an incubator with 5% CO_2 and 37 °C temperature. They were then accurately weighed (W_i : initial weight of vial and gel). Subsequently, 2 mL of D-PBS solutions were applied on top of the hydrogels, which were subsequently incubated at 37 °C. At regular time intervals, the buffer solution was removed from the samples and the hydrogels were weighed (W_t : weight of vial and gel). The percentage of original gel weight remaining is expressed as $(W_t - W_v)/(W_i - W_v) \times 100\%$. The medium was replaced after weighing, and experiments were performed in triplicate.

2.3 Gel morphology

The morphology of the chitosan/HA/ Na_2CO_3 gel was examined by SEM. The gel (1 mL) was placed in one well of a 24-well plate, and precooling at –20 °C was immediately carried out for 20 h. It was then lyophilized at –60 °C for 12 h by using a vacuum freeze-drier. The dried gels were cut with a sharp blade to expose the internal microstructure, placed on double-sided tape, and sputter-coated with gold for SEM at 5.0 kV by using a Hitachi scanning electron microscope (BACPCS4800, Hitachi, Japan). The surface and longitudinal sections were observed.

2.4 Characterization

TEM. Freeze-dried chitosan/HA/ Na_2CO_3 gels were treated at 300, 600, and 1000 °C for 10 h, ground to powders, and then dispersed in ethanol. A drop of the resulting suspension was placed on a carbon-coated copper electron microscope grid and was observed in bright-field TEM mode under a transmission electron microscope (Tecnaï G2 F30, FEI, the Netherlands) operating at an accelerating voltage of 300 kV.

EDS. The elemental composition was measured by EDS coupled with TEM.

2.5 X-ray diffraction

Non-heated samples. The lyophilized chitosan/HA/ Na_2CO_3 gel samples were examined by XRD at room temperature on a Bruker AXS D8 Focus X-ray diffractometer with a Cu K_α radiation source and a LynxEye position-sensitive detector. The X-ray diffractometer was operated at 40 kV and 40 mA. XRD patterns were collected at a 2θ range of 5°–80°, with a step size of 0.02° and a count time of 0.02 s per step.

Heated samples. Selected samples were treated at 1000 °C for 10 h and then ground to powder before analysis. Heat treatment was carried out by using a quartz tubular furnace with nitrogen flow at room temperature to 1000 °C at a heating rate of 2 °C min^{-1} ; the cooling rate was 4 °C min^{-1} . The powders were then analyzed by XRD and compared against the non-heated samples.

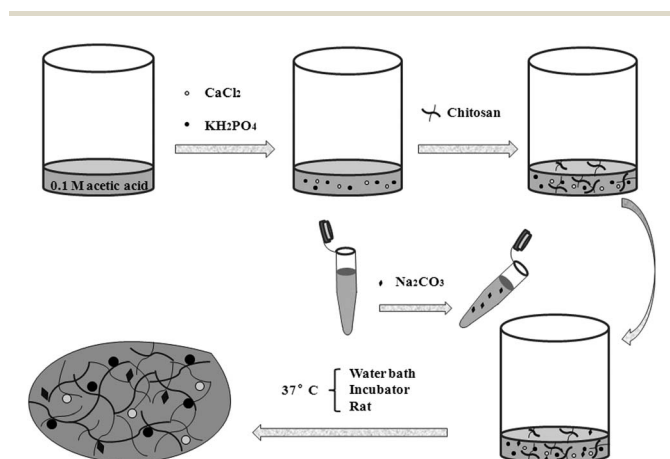


Fig. 1 Simplified cartoon shows how chitosan/HA/ Na_2CO_3 gel was prepared.

2.6 Isolation of rBMSCs

All animals used in the study were housed in sterilized cages with sterile food and water and filtered air, and were handled under a laminar flow hood by following aseptic techniques. They were treated in accordance with the Animal Care Guidelines of the Peking University Health Science Center. Primary rBMSCs were purified as described by Zhang.³³ Sprague–Dawley rats (6–8 weeks, ~250 g) were placed in an anesthesia chamber for around two minutes, and then killed by cervical dislocation. The dissected femurs and tibias were immersed in 75% ethanol for a few seconds and then transferred to $1 \times$ D-PBS (Dulbecco's phosphate buffered saline). They were then transferred to a 10 cm dish (Gibco, USA) containing high-glucose Dulbecco's modified Eagle medium (DMEM, Invitrogen, USA) without FBS. Transfer was done in a biosafety cabinet. Two ends of each bone were cut open with a scissor. A 22G needle was attached to a 5 mL syringe and was filled with DMEM. The marrow was flushed into a 50 mL tube by inserting the needle to an open end of the bone. Two replicates were performed on each bone. When all the marrows were obtained, the cells were resuspended. The cell suspension was passed through a 70 μ m cell strainer (BD Falcon, USA) to remove the bone debris and blood aggregates. The cells were centrifuged at 1200 rpm for 5 min and the supernatant was removed by aspiration. The cells were resuspended in 20 mL of MSC medium (DMEM containing 10% fetal bovine serum (FBS, Gibco, USA) and 1% Pen–Strep), and then equally seeded onto two 10 cm culture dishes. The culture dishes were kept at 37 °C and 5% CO₂ in an incubator for 6–8 days. The medium was changed on the first and second days, and then every 2–3 days. Adherent rBMSCs were rinsed thoroughly with PBS and then detached by using 0.05% trypsin–EDTA (Invitrogen, USA) for use in experiments. The rBMSCs used were taken at passages 3–5.

2.7 Culture curve

At passage 3, 100 μ L of medium containing 2.5×10^3 rBMSCs was seeded into a clean 96-well plate (Corning, USA), and the cells were cultured until 7 days ($N = 6$). At 2 h (0 d), and at 1, 2, 3, 4, 5, 6, and 7 d, the medium was removed and cells were washed twice with D-PBS. A 10 μ L cell counting kit-8 (CCK-8, Dojindo, Japan) and 90 μ L D-PBS were used to estimate the optical density (OD) of rBMSCs. After 1 h incubation, the OD at 450 nm was examined by using a universal microplate spectrophotometer (Biotek Instrument, USA). In this assay, the OD varies with the activity of the cells.

2.8 Osteogenic differentiation *in vitro*

After 3–5 passages in the culture medium, 5×10^4 rBMSCs were seeded onto a clean 6-well plate (Corning, USA) and then incubated overnight. The rBMSCs were cultured in osteogenic medium containing DMEM, 10% FBS, 10 mM β -glyceraldehyde-3-phosphate (Sigma, Germany), 60 mM L-ascorbic acid (Sigma, USA), and 10 nM dexamethasone (Sigma, Germany). The osteogenic medium was replaced every 2–3 days. The osteogenic characteristics were identified through the assay of alkaline

phosphatase (ALP) at 2 weeks and by alizarin red staining at 3 weeks.

2.9 Alkaline phosphatase staining and alizarin red staining

At 14 days, osteogenic differentiation and alkaline phosphatase activity were detected by ALP staining. The culture medium was removed, and cells were washed with D-PBS. The cells were incubated in ALP solution (Nanjing Jiancheng Bioengineering Institute, China) for 8–10 min under protection from light, and then washed three times with distilled water. Phase-contrast microscopy was used to observe the cells.

For the bone-nodule formation assay, the mineralized matrix was evaluated by alizarin red staining. At 21 days of osteogenic differentiation, rBMSCs were rinsed with D-PBS and fixed in 10% formaldehyde for 30 min. The cells were incubated in alizarin red (Sigma, USA) solution for 8–10 minutes and then washed three times with distilled water.

2.10 Evaluation of cytotoxicity induced by chitosan/HA/Na₂CO₃ gel

Chitosan powder, KH₂PO₄, CaCl₂, and Na₂CO₃ were sterilized by ultraviolet light for 30 min. Acetic acid (0.1 M) solution in sterile distilled water as well as chitosan/HA/Na₂CO₃ sol containing 1.4% Na₂CO₃ were prepared. Aliquots of the chitosan/HA/Na₂CO₃ sol (50, 100, and 200 μ L per well) were transferred to a 24-well plate (Corning, USA), and then incubated in a 37 °C incubator to gelate for 30 min ($N = 4$). Culture medium (0.5 mL) with 3×10^4 rBMSCs was seeded into each well. The control sample had no gel. At 1 and 4 days, the medium and gel were removed, and the rBMSCs were washed twice with D-PBS. CCK-8 (15 μ L) and D-PBS (135 μ L) were added to each well. After 1 h of incubation, the OD at 450 nm was measured by using a universal microplate spectrophotometer (Bio-Tek Instrument, USA).

2.11 Cell viability assessment of rBMSCs encapsulated in chitosan/HA/Na₂CO₃ gel

A viability study on hydrogel-encapsulated rBMSCs was performed by a live–dead staining assay. rBMSCs at passages 3–5 were used. The preparation of chitosan/HA/Na₂CO₃ sol was the same as that in the cytotoxicity tests. Cells were encapsulated at a density of 3×10^6 cells per mL. Portions of the formed sol (500 μ L, corresponding to 1.5×10^6 cells per gel sample) were transferred to each well of a 24-well plate. After 30 min incubation, the gel formed. Thereafter, all gels were washed three times with the cell culture medium and then cultured in complete medium. The culture medium was changed every 2–3 days. Cell viability measurements ($n = 4$) were conducted at days 1, 4, 7, and 14. Constructs were washed with sterile PBS three times and then incubated for 10 min with 2 μ M calcein-AM (Dojindo, Japan) and 4 μ M PI (Dojindo, Japan) in D-PBS. Afterward, the constructs were washed again and visualized under an Olympus fluorescence microscope (Olympus, Japan) equipped with Meta Image Series software (MetaMorph, Molecular Devices Corporation, USA).

2.12 SEM of rBMSC cells grown in chitosan/HA/Na₂CO₃

The preparation of chitosan/HA/Na₂CO₃ sol was the same as that performed in the cytotoxicity tests. Chitosan/HA/Na₂CO₃ sol (1 mL) was transferred to a 24-well plate, and then incubated for 30 min. Afterward, 3×10^4 rBMSCs and 0.5 mL culture medium were transferred to each well. The medium was replaced every 2–3 days. At 1 and 7 days, the medium was removed and then washed twice with D-PBS, and the cells were then fixed by using 10% formaldehyde solution.

Chitosan/HA/Na₂CO₃ gels seeded with rBMSCs cells were immediately precooled at $-20\text{ }^\circ\text{C}$ for 20 h. They were then lyophilized at $-60\text{ }^\circ\text{C}$ for 12 h in a vacuum freeze-drier. Lyophilized gels were cut with a sharp blade to expose the internal microstructure, placed on double-sided tape, and then sputter-coated with gold for SEM. SEM was performed on a Hitachi scanning electron microscope operating at 5.0 kV (BACPCS4800, Hitachi, Japan).

2.13 *In vivo* injection of chitosan/HA/Na₂CO₃ sol

Chitosan/HA/Na₂CO₃ sol with 1.4% Na₂CO₃ was prepared through the same procedure used in the cytotoxicity tests.

Six Sprague–Dawley rats (6–8 weeks, ~ 250 g) were randomly divided into two groups. They were subcutaneously injected with 1 mL of chitosan/HA/Na₂CO₃ sol on the left dorsal side or abdomen. After 2 h and 3 weeks, the rats were killed, and the chitosan/HA/Na₂CO₃ gel was extracted.

2.14 Implantation and histological analysis of rBMSCs encapsulated in chitosan/HA/Na₂CO₃ sol in nude mice

The preparation of chitosan/HA/Na₂CO₃ sol was the same as that performed in the cytotoxicity tests. Eight athymic BALB/c nude mice at 6 weeks of age were assigned to two different groups. The osteogenic medium was the same as that in the *in vitro* osteogenic differentiation test. Osteogenic medium (100 μL) containing approximately 1.2×10^6 rBMSCs was mixed with 400 μL of chitosan/HA/Na₂CO₃ sol. The suspension of chitosan/HA/Na₂CO₃ sol, rBMSC cells, and osteogenic medium was then loaded in a 1 mL syringe and then injected subcutaneously through a 16G needle into the dorsum of nude mice. A total of 8 injections (Group I, $N = 4$) were performed (two injections per mouse). The control group (Group II, $N = 4$) of nude mice was injected with the chitosan/HA/Na₂CO₃ sol only. All animals were sacrificed 4 weeks after injection. The implants were individually dissected and removed from the subcutaneous dorsum. Afterward, specimens were immediately fixed in 10%

formaldehyde and then embedded in paraffin. Sections were stained with alizarin red and examined under a light microscope.

2.15 Statistical analysis

All data are presented as mean \pm standard deviation. Quantitative results of the study were subjected to analysis of variance (ANOVA). A level of significance of $p < 0.05$ was used to indicate statistical differences between treatment groups.

3 Results

3.1 Preparation of an injectable HA and formation of thermosensitive chitosan gel *in situ*

To form a physical hydrogel, a basic condition is that the initial polymer concentration must be over the critical concentration at chain entanglement temperature.³⁴ In our work, the final concentration of chitosan was always 2% (w/v), which is more than the critical concentration of chitosan that Boucard³⁴ had proved. Table 1 shows the gelation parameters for chitosan/HA/Na₂CO₃ hydrogels formed by using Na₂CO₃ as an initiator. The range of Na₂CO₃ concentrations tested was 1.4–1.8%. Fig. 2(c) shows that a concentration of 1.4% produced the best solid gel. The control sample with 0% Na₂CO₃ did not undergo sol–gel phase change and remained as a solution until the end of the observation. The concentration and amount of acetic acid solutions in all groups were 0.1 M and 4 mL, respectively. Fig. 2(a and b) show images of the lyophilized chitosan/HA/Na₂CO₃ gel (a) and of rBMSCs seeded onto chitosan/HA/Na₂CO₃ gel and cultured for 7 days (b). Na₂CO₃ concentrations were 1.4%. All dried chitosan gels maintained their columnar and porous characteristics.

3.2 Gelation time

In order to observe the sol–gel phase change behavior of chitosan solutions at physiological body temperature, we measured the gelation time in a $37\text{ }^\circ\text{C}$ water bath by the test-tube inversion method. Fig. 3(a) shows the gelation time of chitosan hydrogel formed at different Na₂CO₃ concentrations. All groups could form chitosan gels at specific durations. With 21.5 mg of KH₂PO₃ and 30 mg of CaCl₂ in 4 mL of 0.1 M acetic acid solution, the chitosan concentration in solution was 2%. With 1.4%, 1.6%, and 1.8% Na₂CO₃, a hydrogel was formed in approximately 8 min. Increasing the polymer concentration from 1.4 to 1.8 wt% and maintaining the other reaction

Table 1 Gelation parameters for chitosan/HA/Na₂CO₃ gels formed by using Na₂CO₃ as an initiator

Trials	Chitosan/HA solution			Chitosan (mg)	Na ₂ CO ₃ solution		%
	Acetic acid (mL)	KH ₂ PO ₃ (mg)	CaCl ₂ (mg)		Acetic acid (mL)	Na ₂ CO ₃ (mg)	
Control	4	21.5	30	100	1	0	0
A	4	21.5	30	100	1	70	1.4
B	4	21.5	30	100	1	80	1.6
C	4	21.5	30	100	1	90	1.8

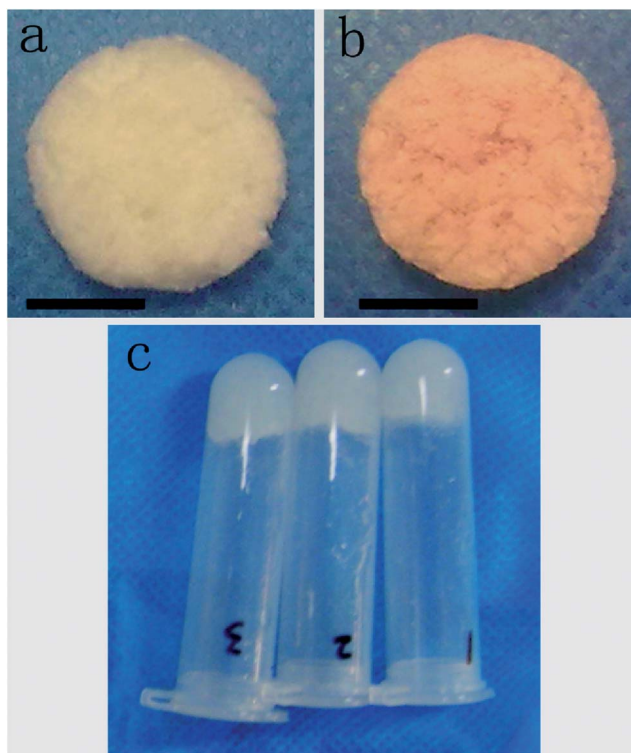


Fig. 2 Images of lyophilized chitosan/HA/Na₂CO₃ gel (a) and rBMSCs seeded onto chitosan/HA/Na₂CO₃ gel and cultured for 7 days (b). Formation of chitosan/HA/Na₂CO₃ gels was promoted with 1.4% Na₂CO₃. Na₂CO₃ concentration was 1.4% (c). The scale bars are 5 mm.

conditions resulted in minimal decrease in gelation time (from 9 to 7 min, Fig. 3(a)).

3.3 Degradation *in vitro*

Degradation of chitosan/HA/Na₂CO₃ gels as a function of incubation time in PBS at 37 °C was monitored (results are shown in Fig. 3(b)). The ratio of Na₂CO₃ had a significant

influence on weight loss. Chitosan gels with Na₂CO₃ concentrations of 1.6% and 1.8% showed a similar rate of weight loss because of less cross-linking; they dissolved significantly faster than did gels with 1.4% Na₂CO₃, and centralized in 1–7 days. All three groups lost their weight steadily up to 30 days (Fig. 3(b)). Chitosan gels with less Na₂CO₃ showed a lower rate of weight loss than that of gels with more Na₂CO₃. At day 30, the weights of chitosan gels with 1.4%, 1.6%, and 1.8% Na₂CO₃ were 43.95%, 38.22% and 37.42%, respectively.

3.4 Gel morphology

The gelation process might involve the formation of characteristic structures at multiple length scales. Thus, we also examined the morphology of chitosan gels at a more global scale by SEM to establish the hierarchical structure of the gels as well as the gelation mechanism. Fig. 4(a and b) show a SEM micrograph of the chitosan gel after water removal by lyophilization. A network structure with interconnected macrodomains composed of the polymer and the pores originally occupied by water was observed. The sizes of the pores were around 20–80 μm.

From the SEM image of the cross-sectional morphologies of freeze-dried chitosan/HA/Na₂CO₃ gels with 1.4% Na₂CO₃ (Fig. 4(c–e)), we could see nanoparticles, some of which were rhombohedral. These might be nano-hydroxyapatite particles formed *in situ*. Small mineral particles coating the gel network is an interesting phenomenon, which is useful in the design of the network structure.

3.5 TEM and EDS

Nano-hydroxyapatite particles of chitosan/HA/Na₂CO₃ gel were visualized by bright-field TEM to observe more closely their morphology and crystal size. Heat treatment at 300, 600, and 1000 °C was done in order to remove the chitosan. Representative TEM micrographs after heat treatment are shown in Fig. 5. The dispersion after heat treatment was more uniform at

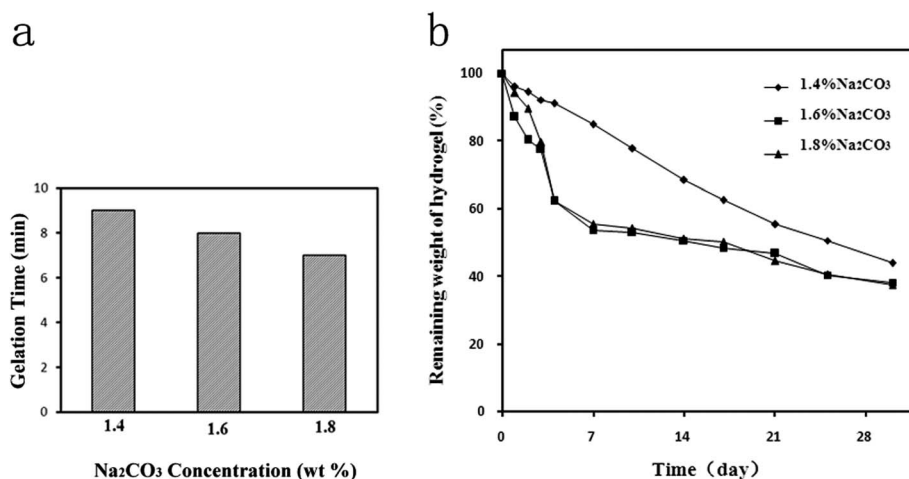


Fig. 3 Gelation times of chitosan/HA/Na₂CO₃ gels formed by using 1.4%, 1.6%, and 1.8% Na₂CO₃ (a). Degradation time of chitosan/HA/Na₂CO₃ gels in PBS at different Na₂CO₃ concentrations at 37 °C *in vitro* (b). Values are reported as averages (N = 3).

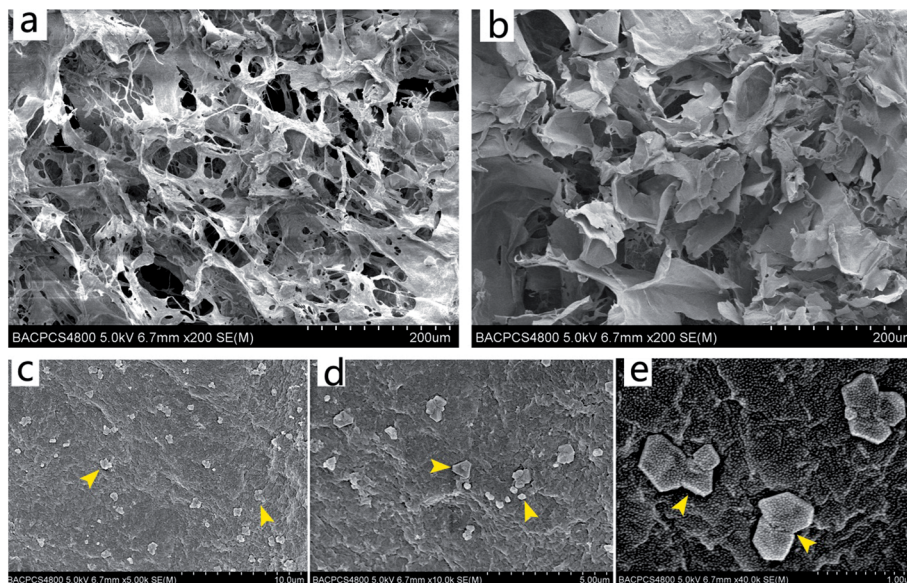


Fig. 4 SEM images of the surface (a) and cross-sectional (b–e) morphologies of freeze-dried chitosan/HA/Na₂CO₃ gels with 1.4% Na₂CO₃. The yellow arrows indicate possible hydroxyapatite nanoparticles. Magnifications are (a and b) 200 \times , (c) 5000 \times , (d) 10 000 \times , and (e) 40 000 \times ; scale bars are (a and b) 200 μ m, (c) 10 μ m, (d) 5 μ m, and (e) 1 μ m.

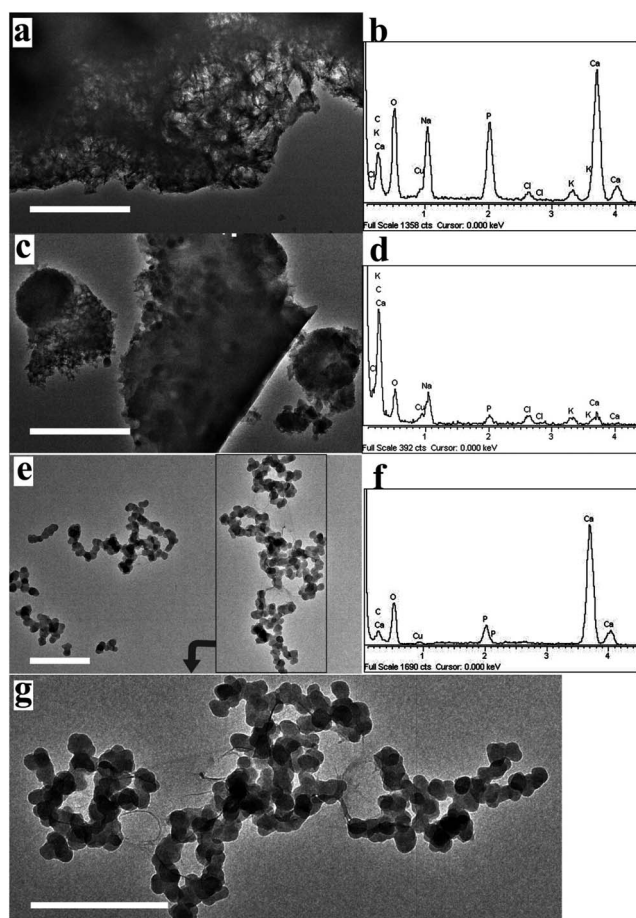


Fig. 5 Bright-field TEM micrographs of freeze-dried chitosan/HA/Na₂CO₃ gels after heat treatment at 300 $^{\circ}$ C (a), 600 $^{\circ}$ C (c) and 1000 $^{\circ}$ C (e and g). Corresponding EDS spectra are shown on the right (b, d and f). Magnifications are (a) 3900 \times , (c) 12 000 \times , and (e and g) 5000 \times ; all scale bars are 500 nm.

1000 $^{\circ}$ C (Fig. 5(e and g)) than at 300 $^{\circ}$ C (Fig. 5(a)) and 600 $^{\circ}$ C (Fig. 5(c)) probably because of complete combustion of the polymer at 1000 $^{\circ}$ C. Nearly spherical particles of 50–100 nm size could be seen very clearly after heat treatment at 1000 $^{\circ}$ C.

Table 2 shows the ablation rate of chitosan/HA/Na₂CO₃ gel. The weight loss (ablation rate) of lyophilized chitosan/HA/Na₂CO₃ gels increased with increasing treatment temperature.

Fig. 5(b, d and f) and Table 3 present results of the qualitative analysis of the synthesized material around the dense particles by TEM-EDS. Ca, P, O, C, Na, Cl, and K were detected at 300 and 600 $^{\circ}$ C. At 1000 $^{\circ}$ C, Ca, P, O, and C were still detected, but not Na, Cl, and K.

3.6 XRD

The phases of the mineral crystals produced by *in situ* processing were investigated by powder XRD analysis. Fig. 6 presents the XRD pattern of the synthesized material. The pattern for synthetic hydroxyapatite (JCPDS: 00-009-0432) could be easily identified; the main phase of the product was therefore an apatitic phase.

Extensive broadening and overlapping of diffraction peaks in the XRD pattern of non-heated gel (Fig. 6(a)) indicate that the HA crystals inside the network were small and had low crystallinity, similar to what is found in natural bones.³⁵ To further

Table 2 Weight loss of lyophilized chitosan/HA/Na₂CO₃ gels with temperature

Temperature	Before heating (mg)	After heating (mg)	Decrease (mg)	Ablating rate (%)
300 $^{\circ}$ C	68.0	36.4	31.6	46.47
600 $^{\circ}$ C	65.1	31.7	33.4	51.31
1000 $^{\circ}$ C	66.3	7.6	58.7	88.54

Table 3 TEM-EDS qualitative analysis of the synthesized material after heating at 1000 °C

	Ca	P	O	C	Cu	Na	Cl	K	Total
Analysis(wt%)									
300 °C	24.97	14.34	20.55	13.68	10.62	12.62	1.36	1.87	100
600 °C	2.66	2.15	10.19	43.42	29.81	7.62	2.37	1.77	100
1000 °C	54.45	7.84	21.96	5.68	10.07				100
Analysis(at%)									
300 °C	14.45	10.74	29.79	26.41	3.88	12.74	0.89	1.11	100
600 °C	1.25	1.31	12.02	68.2	8.85	6.25	1.26	0.85	100
1000 °C	37.57	7	37.97	13.07	4.38				100

confirm the mineral phase, the freeze-dried gels were heated at 1000 °C. Diffraction peaks at 2θ values of 25.8° (002), 31.8° (211), and 34° (300) are in good agreement with HA (JCPDS: 00-009-0432). These could be discerned as three individual peaks, which were not possible before heat treatment.

3.7 Osteogenic differentiation *in vitro* and culture curve of rBMSCs

rBMSCs isolated from SD rats proliferated rapidly in complete culture medium. The rBMSC culture was expanded by passaging five times at most. Phase-contrast microscopy revealed that rBMSCs possessed a spindle-shaped morphology and a round, mononuclear phenotype (Fig. 7(a)). Isolated rBMSCs that were cultured in medium until passage 4 showed no mineral deposits (Fig. 7(a)). Alkaline phosphatase (ALP) activity (Fig. 7(b)) and alizarin red (Fig. 8) staining identified the osteogenic characteristics of rBMSCs. ALP, a marker for early osteoblast

differentiation, was observed as a violet stain in rBMSCs grown in osteogenic medium for 14 days (Fig. 7(b)). Alizarin red (Fig. 8) staining revealed calcium nodules as a nacarat color in rBMSCs grown in osteogenic medium for 21 days (Fig. 8).

An s-shaped growth curve based on the CCK-8 assay was constructed to estimate the OD values of rBMSCs (Fig. 9). The growth curve is in accordance with the logarithmic phase. Passage at 1–3 days corresponded to the slow growth stage. Passage at 4–6 days corresponded to the rapid growth stage followed by a plateau stage. With passage, rBMSC proliferation diminished. rBMSCs at passages 3–5 had the strongest proliferative capability.

3.8 Cytotoxicity of chitosan/HA/Na₂CO₃ gels and viability of rBMSCs grown in chitosan/HA/Na₂CO₃ gels

Fig. 10 shows the test results for estimating the cytotoxicity induced by chitosan/HA/Na₂CO₃ gels. In the biocompatibility

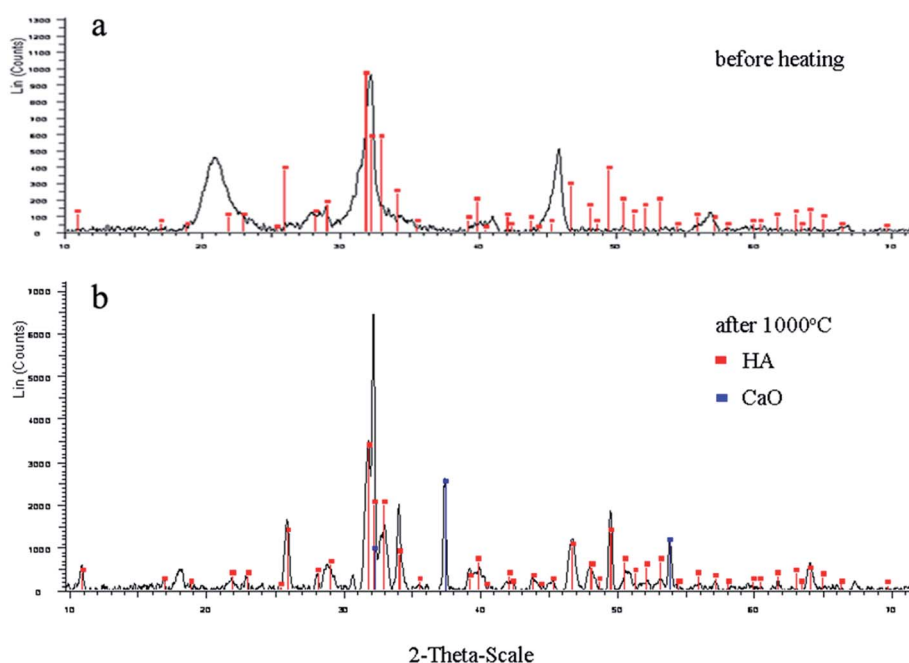


Fig. 6 XRD patterns of freeze-dried chitosan/HA/Na₂CO₃ gels before (a) and after (b) heat treatment at 1000 °C for 10 h. The standard X-ray diffraction pattern of hydroxyapatite (Ca₅(PO₄)₃OH, JCPDS: 00-009-0432) is indicated in red (a and b); that of CaO (b) is indicated in blue. Almost all diffraction lines of the heated gel correspond to hydroxyapatite.

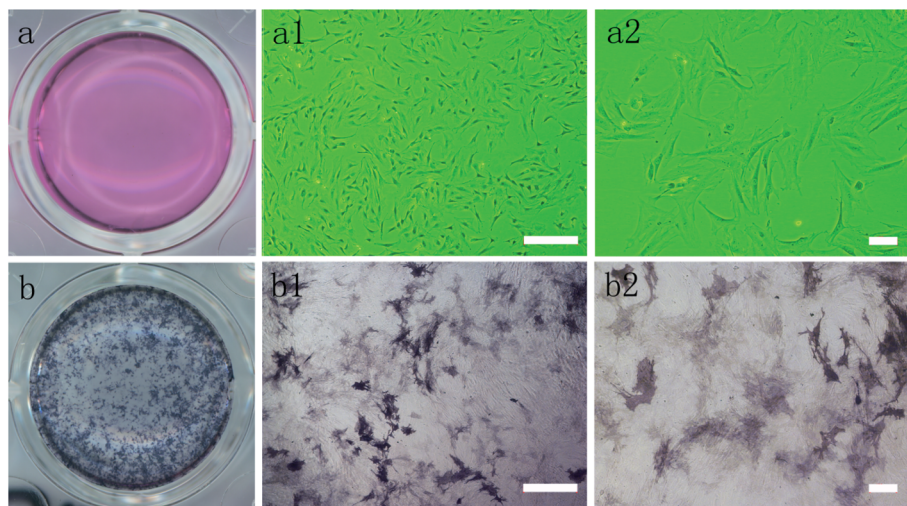


Fig. 7 (a, a1 and a2) Phase-contrast micrographs of rBMSCs isolated from rats at passage 4. (b, b1 and b2) ALP staining at 14 days after *in vitro* osteogenic differentiation of rBMSCs. Magnifications are (a1 and b1) 40 \times and (a2 and b2) 100 \times ; scale bars are (a1 and b1) 500 μ m and (a2 and b2) 100 μ m.

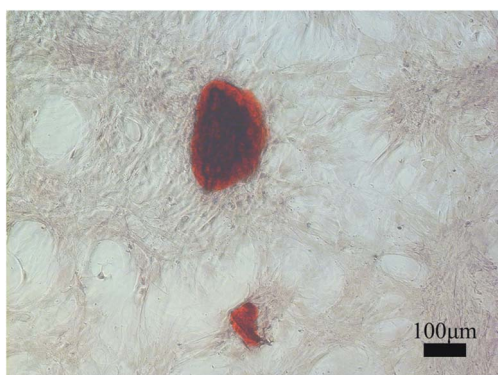


Fig. 8 Alizarin red staining at 21 days after *in vitro* osteogenic differentiation of rBMSCs. Magnification is 100 \times ; scale bar is 100 μ m.

study, the OD values of rBMSCs increased until 4 days on both the chitosan gel ($p < 0.05$) and the tissue culture plate (control). There were significant differences in the amounts of chitosan

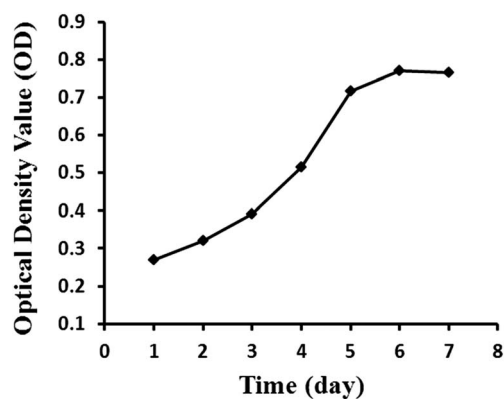


Fig. 9 Growth curve of rBMSCs at passage 3. Cell seeding density: 2.5×10^5 per well. The OD values were estimated by performing CCK-8 assay ($N = 6$).

gel at 4 days, and the OD values decreased along with the increase in the amount of gel.

rBMSCs were incorporated in the gels during the gel preparation. The hydrogel/cell constructs were cultured in medium without differentiation factors for up to 14 days. The viability of rBMSCs encapsulated in the chitosan/HA/ Na_2CO_3 gels was evaluated by live-dead dye staining at predetermined times. Most of the rBMSCs remained viable in the chitosan/HA/ Na_2CO_3 gels immediately after encapsulation and during the 14-day culture period. In this qualitative method, living and dead cells show green and red stains, respectively, under a

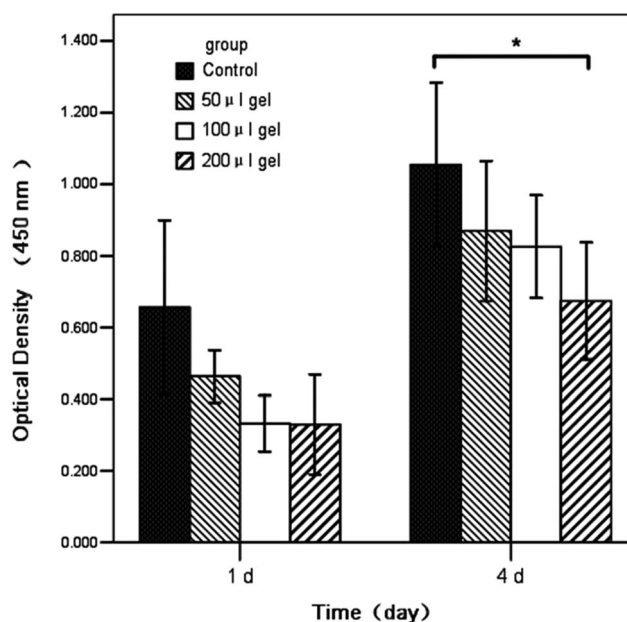


Fig. 10 Viability of rBMSCs measured by CCK-8 assay. rBMSCs grown on a normal culture plate were used as control. Statistical analysis was performed by one-way ANOVA ($p < 0.05$).

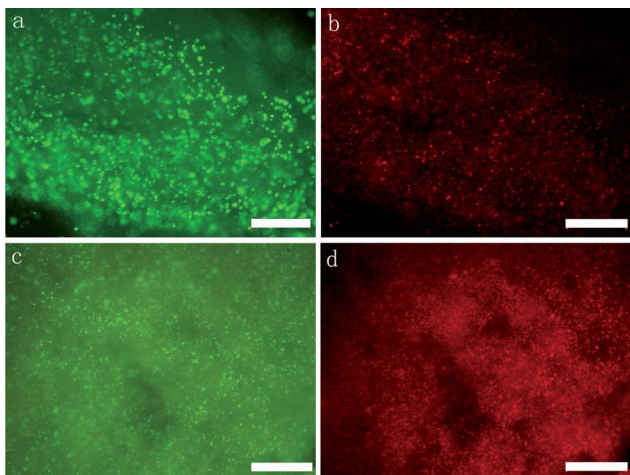


Fig. 11 Fluorescence-microscopy images depicting the viability of rBMSCs encapsulated in chitosan/HA/Na₂CO₃ gel at 1 day (a and b) and 14 days (c and d). Calcein-AM and PI live–dead stain assay: (a) and (c) are green, live cells and (b) and (d) are red, dead cells. Magnifications are 40×; all scale bars are 500 μm.

fluorescence microscope (Fig. 11). When the rBMSCs were encapsulated, the cells were well distributed in the chitosan gel. At day 1 (Fig. 11(a and b)), most cells survived the gel fabrication process. However, the density of live rBMSCs in the chitosan gel at day 14 (Fig. 11(c and d)) was lower than that at day 1. In contrast, the number of dead cells increased at day 14. Fig. 11 reveals that for both culture periods, predominantly living cells were present within the chitosan gels. These results indicate that the chitosan gels might have a slight degree of cytotoxicity. Cells in the chitosan gels maintained a rounded morphology with little evidence of interaction with the surrounding matrix. Thus, the gelation process did not compromise cell viability and there was sufficient mass transport of nutrients and oxygen to the rBMSCs inside the chitosan gel matrix.

3.9 SEM of rBMSCs seeded onto chitosan/HA/Na₂CO₃ gel

rBMSCs at day 1 still maintained a round morphology, as evidenced by SEM observations (Fig. 12(b)). They did not attach to chitosan gels. Importantly, rBMSCs attached and spread on the chitosan gels as culture continued to 7 days (Fig. 12(c and d)). This behavior revealed that the chitosan/HA/Na₂CO₃ gel had a good biocompatibility and might be a suitable cellular framework for bone tissue engineering.

3.10 *In vivo* gelation

We carried out subcutaneous injections of the chitosan/HA sols on the dorsum (2 h) and abdomen (3 weeks) to validate their *in situ* gelling properties.

At 2 h post-injection, the gels formed *in situ* were retained within the subdermal mucous layer (Fig. 13(d)). We killed the SD rats and extracted the gels. All gel samples maintained a beanlike shape and a smooth surface. No swelling and inflammation were detected at the injection sites of chitosan/HA/Na₂CO₃ sols.

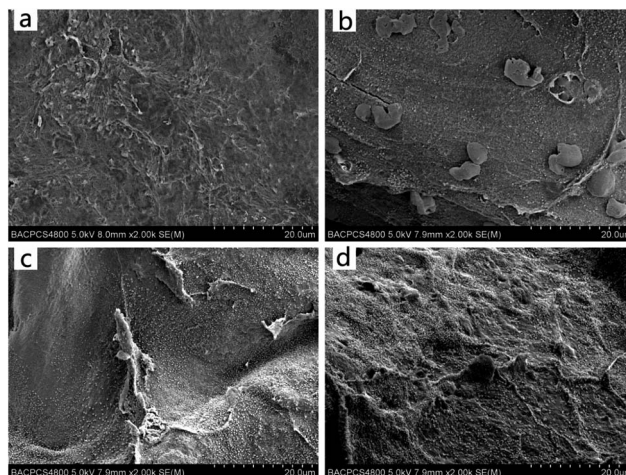


Fig. 12 SEM image of the surface morphology of freeze-dried chitosan/HA/Na₂CO₃ gel without rBMSCs (a). SEM images depicting the morphologies of rBMSCs seeded onto the surface of chitosan/HA/Na₂CO₃ gels after 1 day (b) and 7 days (c and d) of culture. Cell seeding density: 3×10^4 mL gel per well. Magnifications are 2000×; scale bars are 20 μm.

Fig. 13(e and f) show that gels formed after subcutaneous injection maintained their shapes even after 3 weeks. The swelling and inflammation were still absent after a long period.

3.11 Implantation in nude mice

We validated the feasibility of using injectable chitosan sol for *in situ* gelation of the scaffold *in vivo*. Chitosan sol at room temperature containing 3×10^6 rBMSCs, 1.4% Na₂CO₃, and

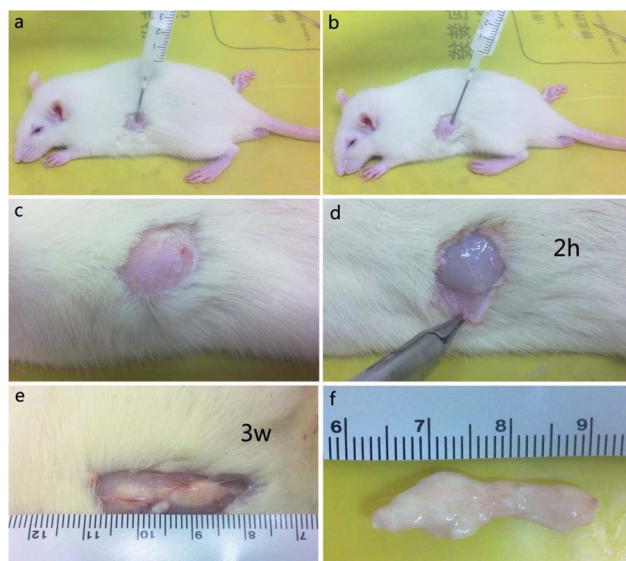


Fig. 13 SD rats injected with 1 mL of chitosan/HA/Na₂CO₃ sol. Images (a) before, (b) during, (c) immediately after, (d) 2 hours after, and (e) 3 weeks after injection. (f) The implant removed from the subcutaneous part of the abdomen. The 2 h assay was performed subcutaneously on the dorsum and the 3-week assay was performed subcutaneously on the abdomen.



Fig. 14 *In situ* formation of chitosan/HA/Na₂CO₃ gel encapsulating rBMSCs. (a) Chitosan/HA/Na₂CO₃ sol with 1.4% Na₂CO₃ and (b and c) at 4 weeks after subcutaneous injection. (c) The white gel formed in a nude mouse.

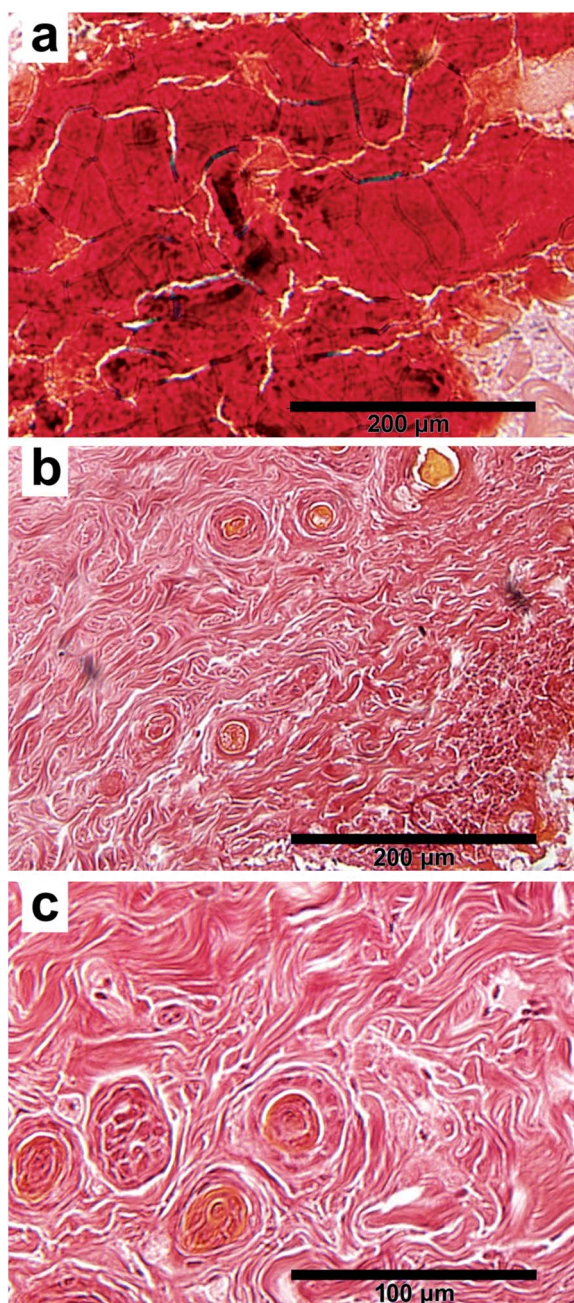


Fig. 15 Alizarin red staining of (a) chitosan/HA/Na₂CO₃ gel (control group) and (b and c) chitosan gel loaded with osteogenic medium and seeded with rBMSCs. Na₂CO₃ concentration was 1.4%. Magnifications are (a and b) 100 \times and (c) 200 \times ; scale bars are (a and b) 200 μ m and (c) 100 μ m.

osteogenic medium was injected subcutaneously into the dorsum of nude mice. Fig. 14 reveals *in situ* chitosan gel formation at 4 weeks after injection.

Histological sections of the chitosan gel implants at 4 weeks were stained by using alizarin red to monitor mineralized bone formation associated with osteogenic differentiation of rBMSCs (Fig. 15). The image of the stained implants containing chitosan gel alone (control group) revealed no mineralization and new vessels (Fig. 15(a)). Furthermore, there were cracks within the chitosan gel. In contrast, new vessels and seeded rBMSCs were seen in the chitosan gel (Fig. 15(b)). Infiltration of inflammatory cells is visible on the edge of the image in Fig. 15(b). No definite evidence of mineral deposition was found.

4 Discussion

Chitosan is a linear polysaccharide composed of randomly distributed β -(1,4)-linked D-glucosamine and N-acetyl-D-glucosamine units (Fig. 1). This polymer is distinct from other commonly available polysaccharides because of the presence of nitrogen in its molecular structure, its cationic character, and its capacity to form polyelectrolyte complexes. Chitosan hydrogels with various shapes, geometries, and formulations (including liquid gels, powders, beads, films, tablets, capsules, microspheres, microparticles, sponges, nanofibrils, textile fibers, and inorganic composites) have been prepared.³⁶ In each preparation, chitosan is either physically associated or chemically cross-linked to form the hydrogel. *In situ* gel-forming scaffolds may be candidates for workable, systemic, and minimally invasive scaffolds.³⁷ An injectable hydrogel is clinically useful, as this system could be used in minimally invasive surgeries. In this study, a new injectable *in situ* forming hydroxyapatite and thermosensitive chitosan gel promoted by Na₂CO₃ was prepared. It may be used as an injectable scaffold for tissue repair.

There are many other methods for synthesizing thermosensitive chitosan gels such as glycerol phosphate disodium salt (GP),^{14,16} pluronic,³⁸ poly(ethylene glycol),³⁹ and poly(lactide-co-glycolide)⁴⁰. These methods need an organic polymer or magnetic stirring at low temperature for copolymerization. In contrast, our hydrogel was obtained by cross-linking of chitosan with Na₂CO₃ at a relatively stable physiological body temperature, with CO₂ as the only byproduct. An organic polymer and low temperature were not required to prepare the chitosan sol. Wang *et al.* developed chitosan and collagen composite hydrogels and verified that collagen-containing materials promoted spreading of embedded cells.⁴¹ Just chitosan gel might not promote spreading of embedded cells.

When Na₂CO₃ was added to chitosan/HA sol and the mixture was heated to 37 $^{\circ}$ C, cross-linking throughout the solution occurred, forming the gel. We chose three different concentrations of Na₂CO₃ (1.4%, 1.6%, and 1.8%) to prepare the chitosan gels (Table 1). In this study, the concentration of Na₂CO₃ had little effect on the gelation time, that is, the gelation time for all three groups was within 7–9 min (Fig. 3(a)). However, the gelation time shortened with the increase in Na₂CO₃ concentration. When 2% Na₂CO₃ was used, the gelation time

was about 6 min and the gel was inhomogeneous. In a preliminary experiment, 1.2% and 1% Na₂CO₃ were used. Here, the gelation times were found to be more than 10 min and the gel strength decreased. Consequently, we chose 1.4% Na₂CO₃ concentration.

Hydrogels prepared by aggregation of chitosan-based copolymers or by neutralization with polyol salts show promising thermoreversible gelation properties in aqueous media.^{16,42} Ionic complexes of mixed-charge systems can be formed between chitosan and small anionic species such as sulfates, citrates, and phosphates.^{43,44} The mechanism of promotion of gelation by Na₂CO₃ may be neutralization of the chitosan sol, with CO₃²⁻ as the anionic crosslinking agent.

Usually, implantation of a biomaterial results in an acute inflammatory response. This occurs most often in biodegradable biomaterials and precedes chronic inflammation.⁴⁵ Reaction to a foreign body (an implanted material) follows a typical sequence of events:^{46,47} of nonspecific adsorption of protein and adhesion of cells (such as monocytes, leukocytes, and platelets) on the biomaterial surface, which lead to giant cell formation and cytokine release. Ultimately, the implant is encapsulated in a fibrous capsule.⁴⁸ The inflammatory phase is a prerequisite to healing.⁴⁹ The implant subcutaneously extracted from nude mouse and stained with alizarin red showed a number of inflammatory cells on the chitosan gel surface and infiltrating the material. In contrast, no inflammatory cells infiltrated when only chitosan gel was used.

The surface and cross-sectional SEM images of the freeze-dried chitosan gels (Fig. 4(a and b)) demonstrate that the chitosan gel had a porous and netlike structure. However, further measures must be taken to verify whether the granules seeded in Fig. 4(c, d and e) are hydroxyapatite nanoparticles. The porous structure provided an environment suitable for the attachment, growth, and differentiation of implanted rBMSCs, and transport of nutrients to the implanted cells.

The XRD pattern of the gel heated at 1000 °C suggests that CaO was incorporated into the powder. As CaO was a calcination product of Ca²⁺ in gel cross-linking, it was not present in the samples before heat treatment. The presence of phosphorus in the gel was confirmed by the XRD results (together with TEM and EDS data, see above), which strongly indicate the presence of hydroxyapatite.

Hydroxyapatite nanoparticles were evenly distributed in the chitosan gel network, which might provide a particularly suitable environment for rBMSC attachment and growth.⁵⁰ Nano-sized HA promotes rBMSC adhesion, differentiation, and proliferation, thus enhancing formation of new bone tissue within a short period.^{51,52}

The HA crystals showed thermal stability and did not decompose into any undesirable secondary phases upon calcination. This makes the composites promising bone-repairing materials and drug- or gene-delivery agents. We will study the contributions of the nanoscale features of these materials to cell responses and mechanical properties.

Cell viability assay and SEM were used to estimate the number of rBMSCs seeded onto the surface of chitosan gels. They clearly showed that the rBMSCs survived and remained

attached on the chitosan gels for at least 14 days. These results suggest that the chitosan gels may be prospective, biocompatible scaffolds for rBMSC attachment and proliferation.

The chitosan gels were then assessed in terms of cell biocompatibility. The rBMSC attachment assay indicated that the hydrogels supported cell adhesion (Fig. 12). A significant number of attached rBMSCs were observed on the surface of hydrogels at 1 or 7 days. Cells seeded on the gel possessed a normal spherical morphology (Fig. 12(b)) similar to that in a normal culture plate.

The osteogenic differentiation of rBMSCs *in vivo* was studied by injecting chitosan sol loaded with osteogenic medium and rBMSCs into nude mice. Many new vessels and inflammatory cells were found in the sections. However, there was no evidence of mineral deposition.

Evaluation of these properties contributes to a further understanding of the formation mechanism and biological applicability of hydrogels. Our process of chitosan gel formation is simple, feasible under mild conditions, and does not employ toxic cross-linking agents such as glyoxal, glutaraldehyde, carbodiimide, and diepoxy compounds. Thus, we believe that such a composite matrix has potential use in tissue engineering, wound management, drug delivery, and other related biomedical applications. However, further optimization of the system is required to promote the mechanical strength to verify the existence of mineral deposition, and to study its uses in bone tissue engineering.

5 Conclusions

Injectable systems for various therapeutic needs are in high demand because of their ease of application, *in situ* gelation, and their ability to decrease patient discomfort.

Chitosan gels were biocompatible with cultured rBMSCs. Encapsulation of rBMSCs demonstrated that the composite hydrogel promoted cell survival and that the cells retained their regular spherical morphology. These preliminary studies indicate that the chitosan/HA/Na₂CO₃ gel supported rBMSCs adhesion and encapsulation, and might have potential use in bone tissue engineering applications.

Acknowledgements

We are grateful to the Peking University School and Hospital of Stomatology for the Postdoctoral Sustentation Fund.

Notes and references

- 1 R. F. Service, *Science*, 2000, **289**, 1498–1500.
- 2 J. S. Tememoff and A. G. Mikos, *Biomaterials*, 2000, **21**, 2405–2412.
- 3 J. L. Drury and D. J. Mooney, *Biomaterials*, 2003, **24**, 4337–4351.
- 4 Q. P. Hou, P. A. De Bank and K. M. Shakesheff, *J. Mater. Chem.*, 2004, **14**, 1915–1923.
- 5 A. B. Pratt, F. E. Weber, H. G. Schmoekel, R. Müller and J. A. Hubbell, *Biotechnol. Bioeng.*, 2004, **86**, 27–36.

- 6 L. Lao, H. Tan, Y. Wang and C. Gao, *Colloids Surf., B*, 2008, **66**, 218–225.
- 7 A. Gutowska, B. Jeong and M. Jasionowski, *Anat. Rec.*, 2001, **263**, 342–349.
- 8 D. J. Park, B. H. Choi, S. J. Zhu, J. Y. Huh, B. Y. Kim and S. H. Lee, *Journal of Cranio-Maxillo-Facial Surgery*, 2005, **33**, 50–54.
- 9 R. Jin, L. S. Moreira Teixeira, P. J. Dijkstra, M. Karperien, C. A. van Blitterswijk, Z. Y. Zhong and J. Feijen, *Biomaterials*, 2009, **30**, 2544–2551.
- 10 H. Tan, C. R. Chu, K. A. Payne and K. G. Marra, *Biomaterials*, 2009, **30**, 2499–2506.
- 11 C. Shi, Y. Zhu, X. Ran, M. Wang, Y. Su and T. Cheng, *J. Surg. Res.*, 2006, **133**, 185–192.
- 12 I. Y. Kim, S. J. Seo, H. S. Moon, M. K. Yoo, I. Y. Park, B. C. Kim and C. S. Cho, *Biotechnol. Adv.*, 2008, **26**, 1–21.
- 13 Y. Zhang and M. Zhang, *J. Biomed. Mater. Res.*, 2001, **55**, 304–312.
- 14 L. Wang and J. P. Stegemann, *Biomaterials*, 2010, **31**, 3976–3985.
- 15 A. Chevrier, C. D. Hoemann, J. Sun and M. D. Buschmann, *Osteoarthritis and Cartilage*, 2007, **15**, 316–327.
- 16 A. Chenite, C. Chaput, D. Wang, C. Combes, M. D. Buschmann, C. D. Hoemann, J. C. Leroux, B. L. Atkinson, F. Binette and A. Selmani, *Biomaterials*, 2000, **21**, 2155–2161.
- 17 K. E. Crompton, J. D. Goud, R. V. Bellamkonda, T. R. Gengenbach, D. I. Finkelstein, M. K. Horne and J. S. Forsythe, *Biomaterials*, 2007, **28**, 441–449.
- 18 K. S. Kim, J. H. Lee, H. H. Ahn, J. Y. Lee, G. Khang, B. Lee, H. B. Lee and M. S. Kim, *Biomaterials*, 2008, **29**, 4420–4428.
- 19 C. Du, F. Z. Cui, W. Zhang, Q. L. Feng, X. D. Zhu and K. de Groot, *J. Biomed. Mater. Res., Part A*, 2000, **50**, 518–527.
- 20 M. Kikuchi, S. Itoh, S. Ichinose, K. Shinomiya and J. Tanaka, *Biomaterials*, 2001, **22**, 1705–1711.
- 21 Z. Ahmad and J. E. Mark, *Mater. Sci. Eng., C*, 1998, **6**, 183–196.
- 22 L. L. Hench, *J. Am. Ceram. Soc.*, 1991, **74**, 1487–1510.
- 23 C. R. Nunes, S. J. Simske, R. Sachdeva and L. M. Wolford, *J. Biomed. Mater. Res., Part A*, 1997, **36**, 560–563.
- 24 M. Ito, *Biomaterials*, 1991, **12**, 41–45.
- 25 T. Kawakami, M. Antoh, H. Hasegawa, T. Yamaguchi, M. Ito and S. Eda, *Biomaterials*, 1992, **13**, 759–763.
- 26 Y. J. Yin, F. Zhao, X. F. Song, K. D. Yao, W. W. Lu and J. C. Leong, *J. Appl. Polym. Sci.*, 2000, **77**, 2929–2938.
- 27 I. Yamaguchi, K. Tokuchi, H. Fukuzaki, Y. Koyama, K. Takakuda, H. Monma and J. Tanaka, *J. Biomed. Mater. Res., Part A*, 2001, **55**, 20–27.
- 28 C. A. W. Andrew, K. Eugene and W. H. Garth, *J. Biomed. Mater. Res., Part A*, 1998, **41**, 541–548.
- 29 T. Taguchi, A. Kishida and M. Akashi, *J. Biomater. Sci., Polym. Ed.*, 1999, **10**, 331–339.
- 30 W. Tachaboonyakiat, T. Serizawa and M. Akashi, *Polym. J.*, 2001, **33**, 177–181.
- 31 M. Xie, M. Ø. Olderøy, J. P. Andreassen, S. M. Selbach, B. L. Strand and P. Sikorski, *Acta. Biomater.*, 2010, **6**, 3665–3675.
- 32 D. Gupta, C. H. Tatorc and M. S. Shoichet, *Biomaterials*, 2006, **27**, 2370–2379.
- 33 L. Zhang and C. Chan, *J. Visualized Exp.*, 2010, DOI: 10.3791/1852.
- 34 N. Boucard, C. Viton and A. Domard, *Biomacromolecules*, 2005, **6**, 3227–3237.
- 35 S. V. Dorozhkin, *J. Mater. Sci.*, 2007, **42**, 1061–1095.
- 36 E. B. Denkbass and R. M. Ottenbrite, *J. Bioact. Compat. Polym.*, 2006, **21**, 351–368.
- 37 K. S. Kim, J. Y. Lee, Y. M. Kang, E. S. Kim, B. Lee, H. J. Chun, J. H. Kim, B. H. Min, H. B. Lee and M. S. Kim, *Tissue Eng., Part A*, 2009, **10**, 3201–3209.
- 38 K. M. Park, S. Y. Lee, Y. K. Joung, J. S. Na, M. C. Lee and K. D. Park, *Acta Biomater.*, 2009, **5**, 1956–1965.
- 39 F. Ganji and M. J. Abdekhodaie, *Carbohydr. Polym.*, 2008, **74**, 435–441.
- 40 F. Ganji and M. J. Abdekhodaie, *Carbohydr. Polym.*, 2010, **80**, 740–746.
- 41 L. Wang and J. P. Stegemann, *Biomaterials*, 2010, **31**, 3976–3985.
- 42 J. P. Chen and T. H. Cheng, *Polymer*, 2009, **50**, 107–116.
- 43 X. Z. Shu and K. J. Zhu, *Int. J. Pharm.*, 2002, **233**, 217–225.
- 44 E. C. Shen, C. Wang, E. Fu, C. Y. Chiang, T. T. Chen and S. Nieh, *J. Periodontal Res.*, 2008, **43**, 642–648.
- 45 G. W. Bos, W. E. Hennink, L. A. Brouwer, W. den Otter, T. F. J. Veldhuis, C. F. van Nostrum and M. J. van Luyn, *Biomaterials*, 2005, **26**, 3901–3909.
- 46 J. M. Anderson, *Annu. Rev. Mater. Res.*, 2001, **31**, 81–110.
- 47 B. D. Ratner and S. J. Bryant, *Annu. Rev. Biomed. Eng.*, 2004, **6**, 41–75.
- 48 J. Kopecek and J. Y. Yang, *Polym. Int.*, 2007, **56**, 1078–1098.
- 49 R. S. Kirsner and W. H. Eaglstein, *Dermatol. Clin.*, 1993, **11**, 629–640.
- 50 J. L. Moreau and H. H. K. Xu, *Biomaterials*, 2009, **30**, 2675–2682.
- 51 T. J. Webster, C. Ergun, R. H. Doremus, R. W. Siegel and R. Bizios, *Biomaterials*, 2000, **21**, 1803–1810.
- 52 X. Liu, L. A. Smith, J. Hu and P. X. Ma, *Biomaterials*, 2009, **30**, 2252–2258.